APD SOLEIL

CNRS/CEA/MESR

APD SOLEIL/A/95-03
Rubrique : Optique

SOLEIL :

OPTICS AND PERFORMANCES OF THE SOURCE

P. Brunelle*, J. Faure**, M.-P. Level*, A. Nadji*, P. Nghiem**, J. Payet**, M. Sommer*, A. Tkatchenko**, H. Zyngier*.

* : LURE, Centre Universitaire, Bât. 209 D, 91405 Orsay Cedex, France.
** : LNS, Centre d'Etudes de Saclay, 91191 Gif sur Yvette Cedex, France.

September 1995

I. INTRODUCTION

From the beginning of the SOLEIL project studies, the specifications have changed continuously [1, 2]. The basic characteristics remain the same, namely a polyvalent synchrotron radiation source in the 10 eV-20 keV energy range with a large number of undulators, a few special 10-20 keV sources and up to 40 beamlines to satisfy the VUV and soft X-rays communities. However, the performances required are now more ambitious such as extremely high brilliance and possible FEL operation. This report discusses the choice of the configuration and presents the performances of the optics for different tunings. Details are given on optical functions, dynamic aperture, injection, stability with high positive vertical chromaticity. The sensitivity to dipolar errors, focusing errors and multipolar field components has also been tested in order to define the tolerances on magnetic fields. Beam lifetime for different tunings, and brilliance calculations for various insertion devices are also presented in this paper.

II. CHOICE OF THE CONFIGURATION

The choice concerns the cell lattice as well as the length and number of long straight sections. Furthermore, as only few 10-20 keV sources are required, short wigglers are preferred rather than superconducting bending magnets, the choice of the configuration takes this into account.

1) Basic cell lattice

Extensive studies have been undertaken in order to choose the best lattice providing the very low emittance ($\approx$ 2 nm.rad) needed to reach the required high brilliance of 10^{20} ph/s/mm^2/mrad^2/0.1 % $\Delta\lambda/\lambda$ from undulators.

In order to allow for a large number of undulators, multiple bend structures were not considered while DB and TB structures were compared as well as bending magnet field index efficiency and various arrangements of multiplets. It turns out that for the same number of periods, TBA and DBA have more or less the same practical minimum emittance, the ratio to the theoretical minimum emittance being larger for the TBA. When the dispersion is distributed, the results are similar. A field index has only a small effect (10 to 20 %) on the value of the final emittance. Both structures require 16 cells in order to reach an emittance around 2 nm.rad. As there is no superconducting bending magnet planned, the simplest DB structure (n = 0) is chosen.

2) FEL dedicated straight section

The aim of the FEL is to provide a powerful tunable (350-100 nm) picosecond source with a practical lifetime (> 10 h) and a reasonable gain (50 %) in order to perform user experiments [3].

The optimized energy of 1.5 GeV results from a compromise between mirror degradation and gain on one hand and laser power and beam lifetime on the other.

Similarly the length of the straight section was determined as a compromise between the maximum length of the insertion device which defines the gain and the stability of the optical cavity. As the FEL is designed for experimental use, the optical cavity mechanics must be outside the shielding for providing various FEL parameters according to the users requirements. Taking into account the deformation due to local heating, the mirror curvature radius cannot be too large (≈ 30 m) in order to keep the cavity stable. This point leads to an optical cavity length of around 40 m and an optimum length for the straight section of 14 m.

3) Number of long straight sections

Different configurations have been studied with 8, 4 and 2 superperiods. As the symmetry order is decreased the optimization of the optics in terms of optical function matching and dynamic aperture becomes more difficult. For 2 superperiods a unit matrix scheme with 6 additional quadrupole families is needed to obtain a good solution with two long straight sections, which increases dramatically the length of the optical cavity. Good results were obtained for 8 superperiods without additional quadrupoles, but the total length of the machine became too large. After a longer optimization a good solution with 4 superperiods was found and retained for SOLEIL. It offers a better solution for the FEL operation (no additional quadrupole) and two long additional straight sections open for future experiments.

III. MACHINE PARAMETERS

The energy for machine operation varies from 1.5 GeV (FEL and temporal structure operation) to 2.15 GeV (high brilliance operation). 8 quadrupole families are used to obtain the required low emittance and low β-functions in medium straight sections. 8 sextupole families are used to compensate for natural chromaticities and to minimize the tune shift variation with both amplitude and energy. **Table 1** shows the main machine parameters given at 2.15 GeV.

Table 1 : Machine parameters.

Energy (GeV)	2.15
Circumference (m)	336
Lattice cell type	DB + 4 long straight sections
Number of cells, number of superperiods	16, 4
Straight section length	14.1 m x 4 + 7.4 m x 12
Dipole : field (T), nb	1.56, 32
Quad. : max gradient (T/m), nb, [nb of families]	18, 160, [8]
Sext. : max strength (T/m^2), nb, [nb of families]	250, 112, [8]
Radiation loss per turn (keV)	410 + 90 [insertion devices]
RF frequency (MHz), max peak voltage (MV)	500, 3

IV. OPTICS RESULTS

All the simulations have been performed with a modified version of the BETA code developped at LNS [4]. A large number of operating points have been studied in order to obtain low emittance and to provide low beta-functions in straight sections for insertion devices [5]. Main optical characteristics and maximum brilliances are given in Appendix A for the eleven optimized operating points. Their location in the tune diagram is shown in **figure 1**. The horizontal emittance is about 7 nm.rad in the Chasman-Green structure and reaches 2.4 nm.rad with distributed dispersion.

A special operating point has been optimized for FEL operation and temporal structure with an emittance of 15 nm.rad at 1.5 GeV, i.e. 30 nm.rad at 2.15 GeV and zero dispersion in the long straight sections [6].

Three nominal operating points have been studied in detail, which emittances are 7.7 nm.rad (Chasman-Green structure), 2.7 nm.rad (high brilliance operation) and 30 nm.rad (FEL operation and temporal structure). The tunes have been chosen below half integer to minimize the resistive wall instability.

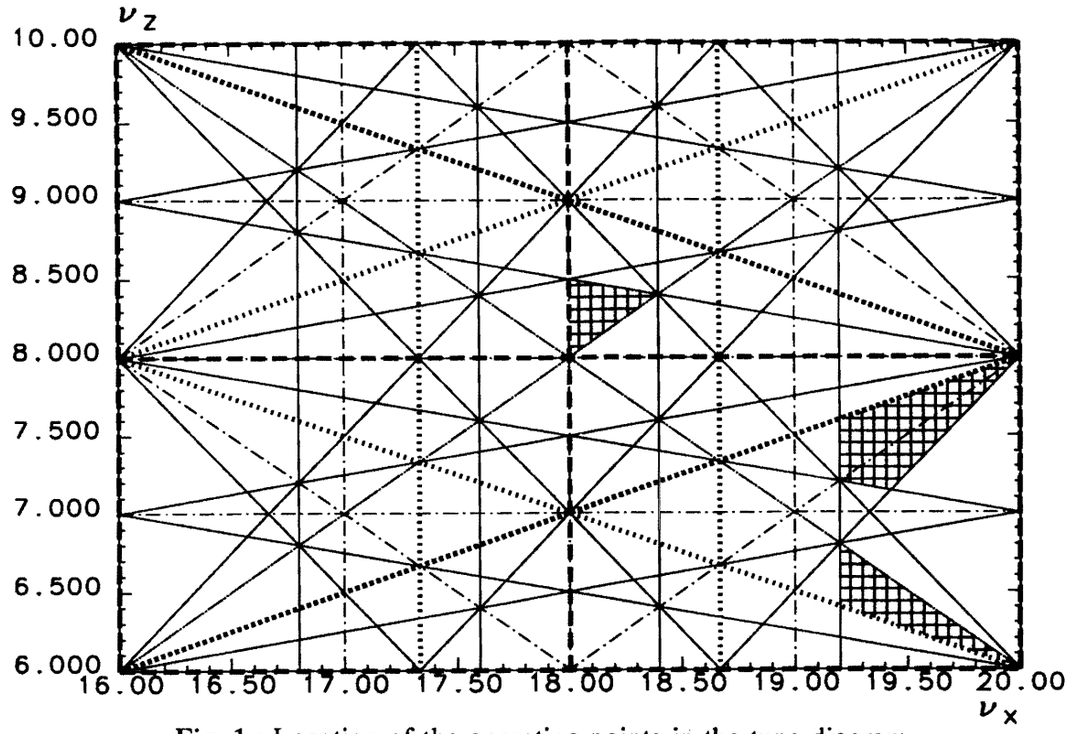

Fig. 1 : Location of the operating points in the tune diagram with systematic resonances from 2nd to 5th order.

1) Optical functions and dynamic aperture

The main characteristics of these 3 operating points are given in **Table 2.**

Table 2 : Nominal operating point characteristics.

Emittance (nm.rad)	2.7	7.7	15
Energy (GeV)	2.15	2.15	1.5
Betatron tunes ν_x, ν_z	18.30, 8.38	18.30, 8.30	19.40, 6.38
Synchrotron tune ν_s	$5.3\ 10^{-3}$	$5.3\ 10^{-3}$	$15.2\ 10^{-3}$
Momentum compaction α	$3.8\ 10^{-4}$	$5.5\ 10^{-4}$	$1.3\ 10^{-3}$
Energy spread σ_ε	$8.6\ 10^{-4}$	$8.6\ 10^{-4}$	$6.0\ 10^{-4}$
Damping times (ms) τ_s, τ_x, τ_z	5.85, 11.7, 11.7	5.85, 11.7, 11.7	17.2, 34.4, 34.4
Natural bunch length (mm), σ_ℓ	3.3	3.3	2.8
V_{RF} (MV) for ε_{RF} = 4 %	1.9	2.4	3
Natural chromaticities (ξ_x, ξ_z)	- 2.98, - 2.90	-3.27, -2.84	- 2.87, - 3.41

The optical functions are given on **figures 2, 3 and 4.** The low β-functions in straight sections are about 3 m and a large β_x-value in the long straight sections (about 15 m) is required for injection.

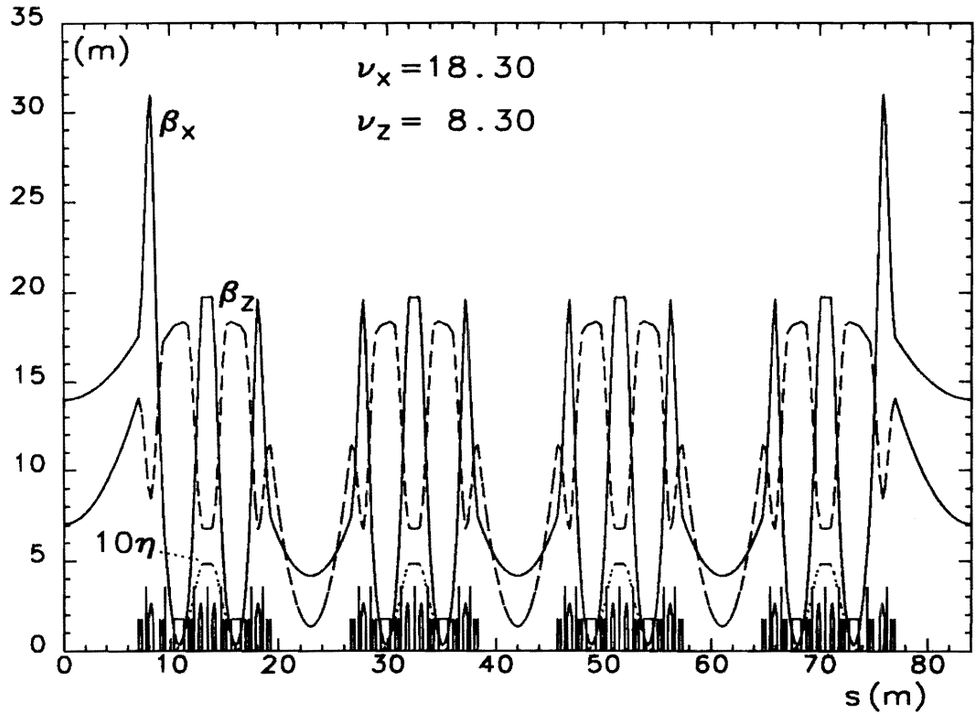

Fig. 2 : Optical functions for ε_x = 7.7 nm.rad.

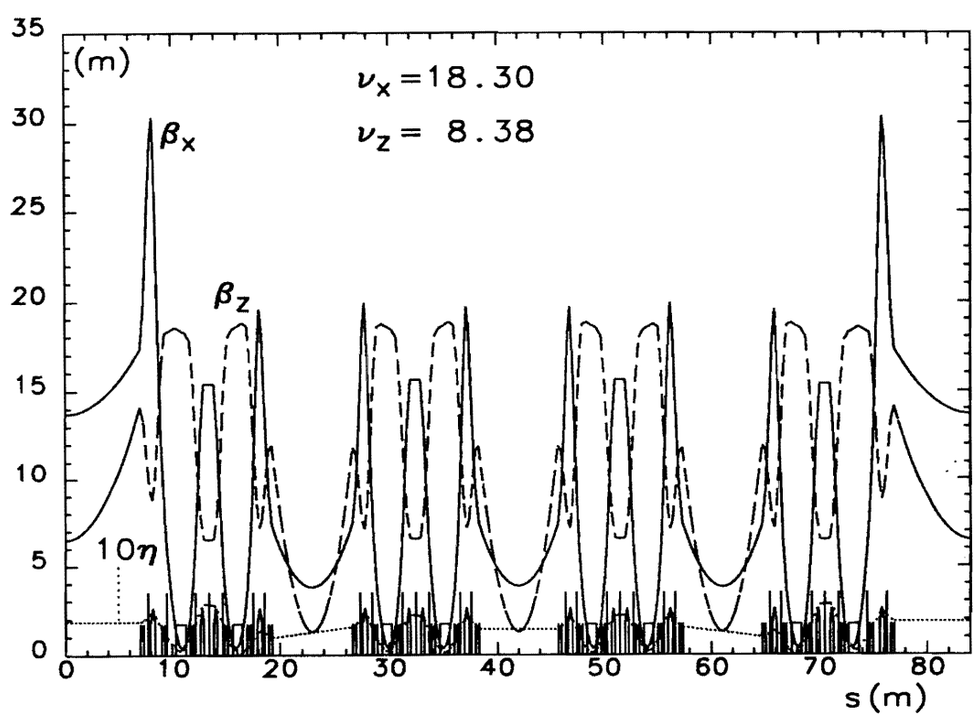

Fig. 3 : Optical functions for ε_x = 2.7 nm.rad.

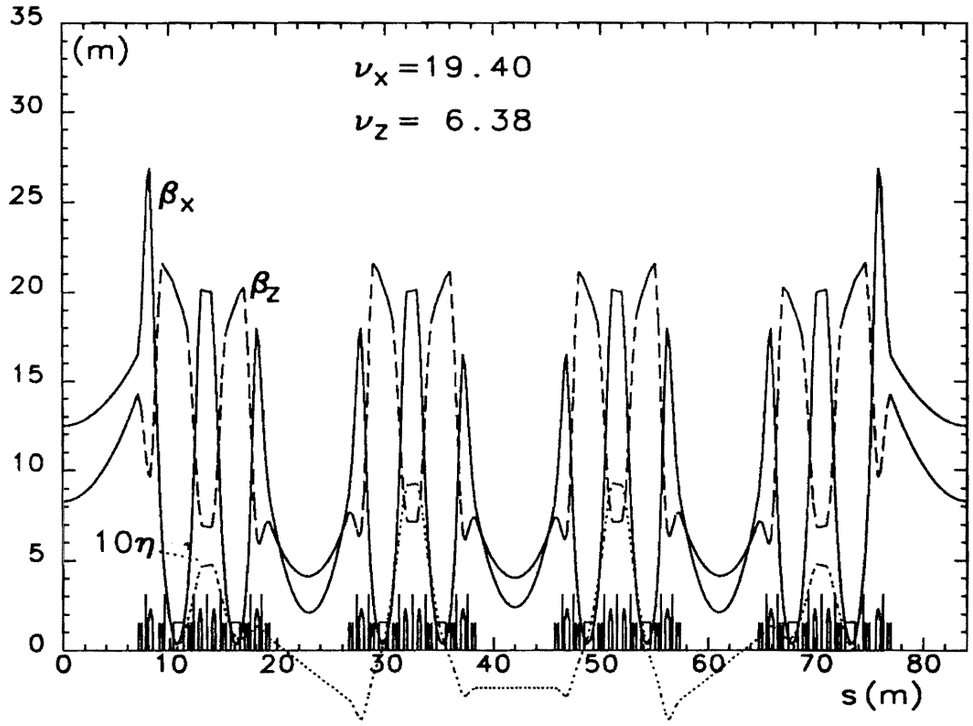

Fig. 4 : Optical functions for $\varepsilon_x = 30$ nm.rad (15 nm.rad at 1.5 GeV).

The corresponding dimensions at source points are given in **Table 3** for the three nominal points with a $\kappa^2 = 1$ % coupling.

Table 3 : Dimensions at source points.

ε_x (nm.rad)	2.7	7.7	15
Long straight section :			
σ_x (µm)	252	328	306
σ'_x (µrad)	14	23	94
σ_z (µm)	13	23	245
σ'_z (µrad)	2	3	60
Medium straight section :			
σ_x (µm)	157	178	185
σ'_x (µrad)	27	43	56
σ_z (µm)	6	10	173
σ'_z (µrad)	5	7	43
Bending Magnet (at 3° port) :			
σ_x (µm)	32	69	88
σ'_x (µrad)	108	185	134
σ_z (µm)	22	37	376
σ'_z (µrad)	1	2	20

The dynamic aperture has been optimised to be comfortable even with an energy deviation up to ± 4 % for $\xi_x = \xi_z = 0$.

The **figures 5, 6 and 7** show the dynamic apertures for $\Delta p/p = 0$ and ± 4 % obtained for the three nominal points.

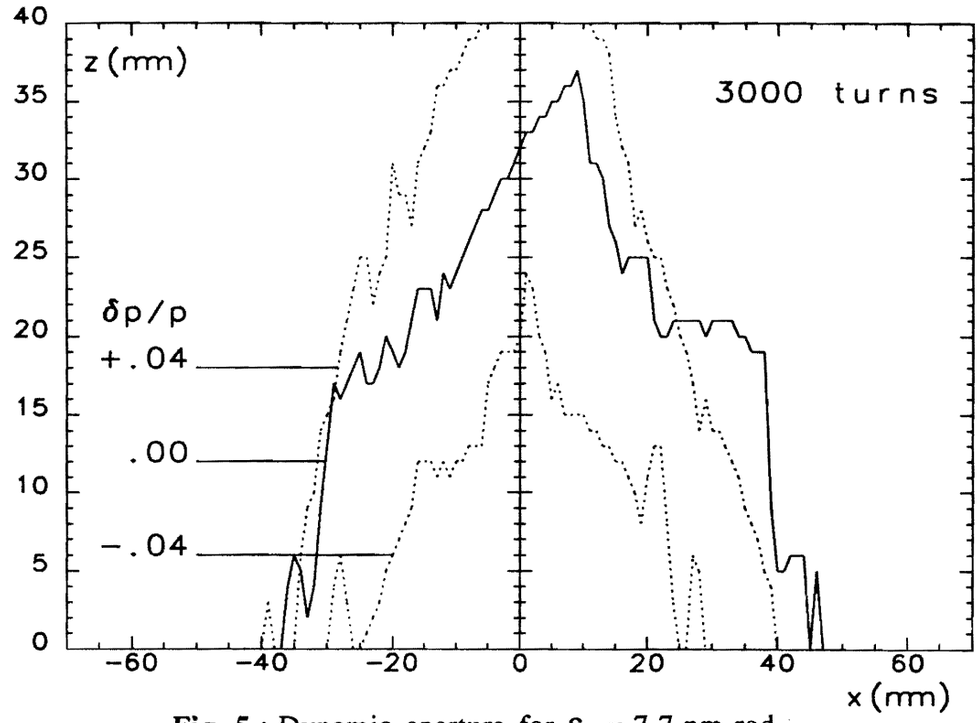

Fig. 5 : Dynamic aperture for ε_x = 7.7 nm.rad.

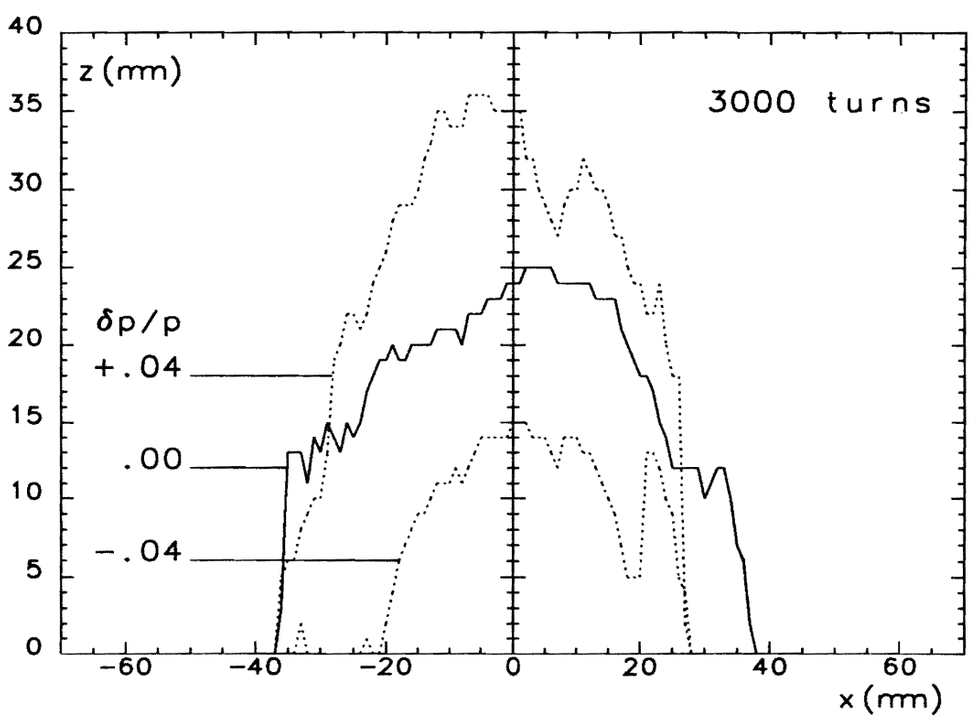

Fig. 6 : Dynamic aperture for ε_x = 2.7 nm.rad.

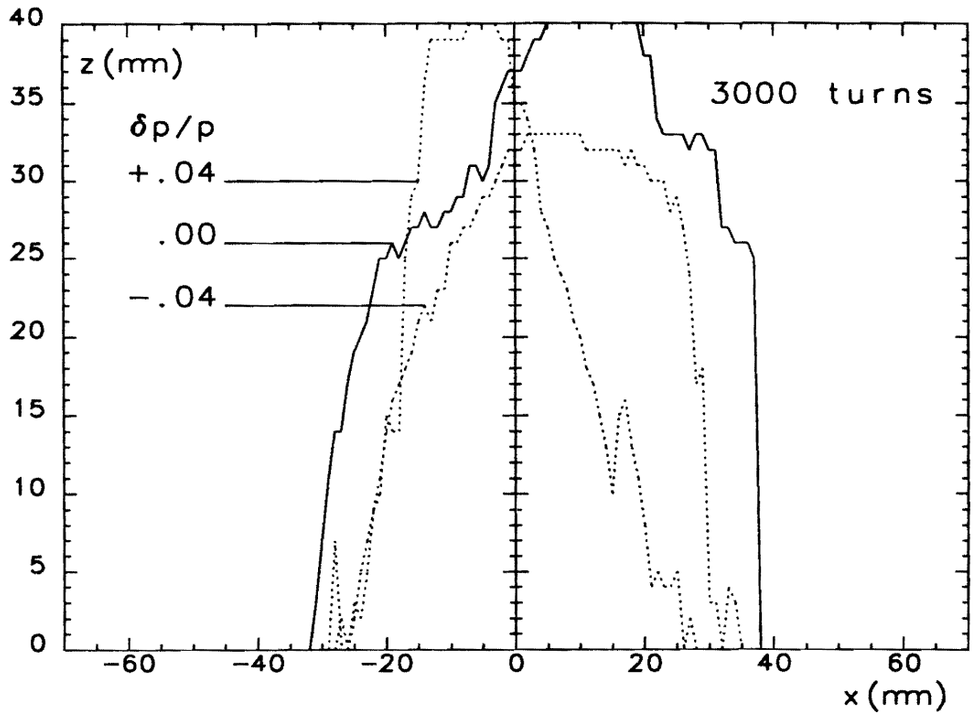

Fig. 7 : Dynamic aperture for ε_x = 30 nm.rad.

As a high positive vertical chromaticity is expected to increase the single bunch current threshold, the dynamic aperture has been optimised also for $\xi_z = +1$ [7]. The larger sextupole strengths lead to a reduced dynamic aperture and then to a smaller energy acceptance. The study of the nominal points has shown that the dynamic aperture remains comfortable only if $\Delta p/p \leq 1.5$ % because of the strong variation of the vertical tune with energy.

The dynamic aperture obtained for the nominal point $\varepsilon_x = 2.7$ nm.rad with $\Delta p/p = 0$ and $\pm$ 1.5 % is given on **figure 8**.

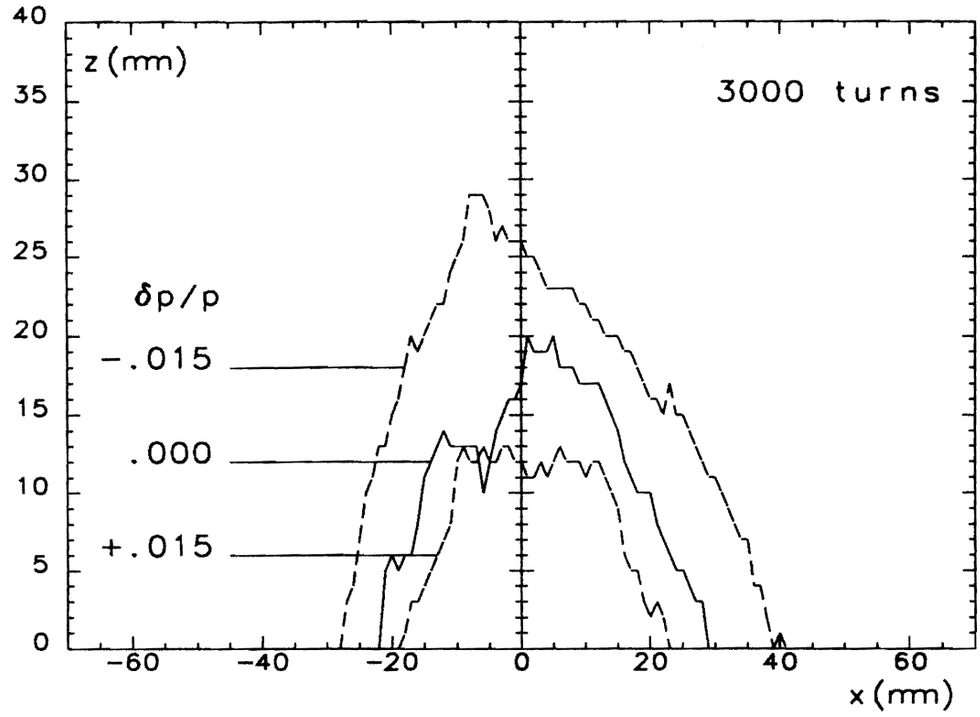

Fig. 8 : Dynamic aperture for $\varepsilon_x = 2.7$ nm.rad and $\xi_z = +1$.

2) Sensitivity to dipolar errors

The sensitivity of all the optics has been tested versus standard dipolar errors [8]. This yields to the following tolerances given as r.m.s. values.

- Integrated field error :
  - dipoles : $\sigma(B\ell)/(B\ell)_0 = 1\ 10^{-3}$

Nevertheless, considerations about closed orbit correction lead to choose a more stringent tolerance : $\sigma(B\ell)/(B\ell)_0 = 5\ 10^{-4}$ [9].

- Alignment errors :
  - dipoles : $\sigma_s = 5\ 10^{-4}$ m
    $\sigma_z = 5\ 10^{-4}$ m
    $\sigma_{\theta s} = 2\ 10^{-4}$ rad
  - quadrupoles : $\sigma_x = 1\ 10^{-4}$ m
    $\sigma_z = 1\ 10^{-4}$ m

The effect on closed orbit is given on **figure 9** for the operating point $\varepsilon_x = 2.7$ nm.rad.

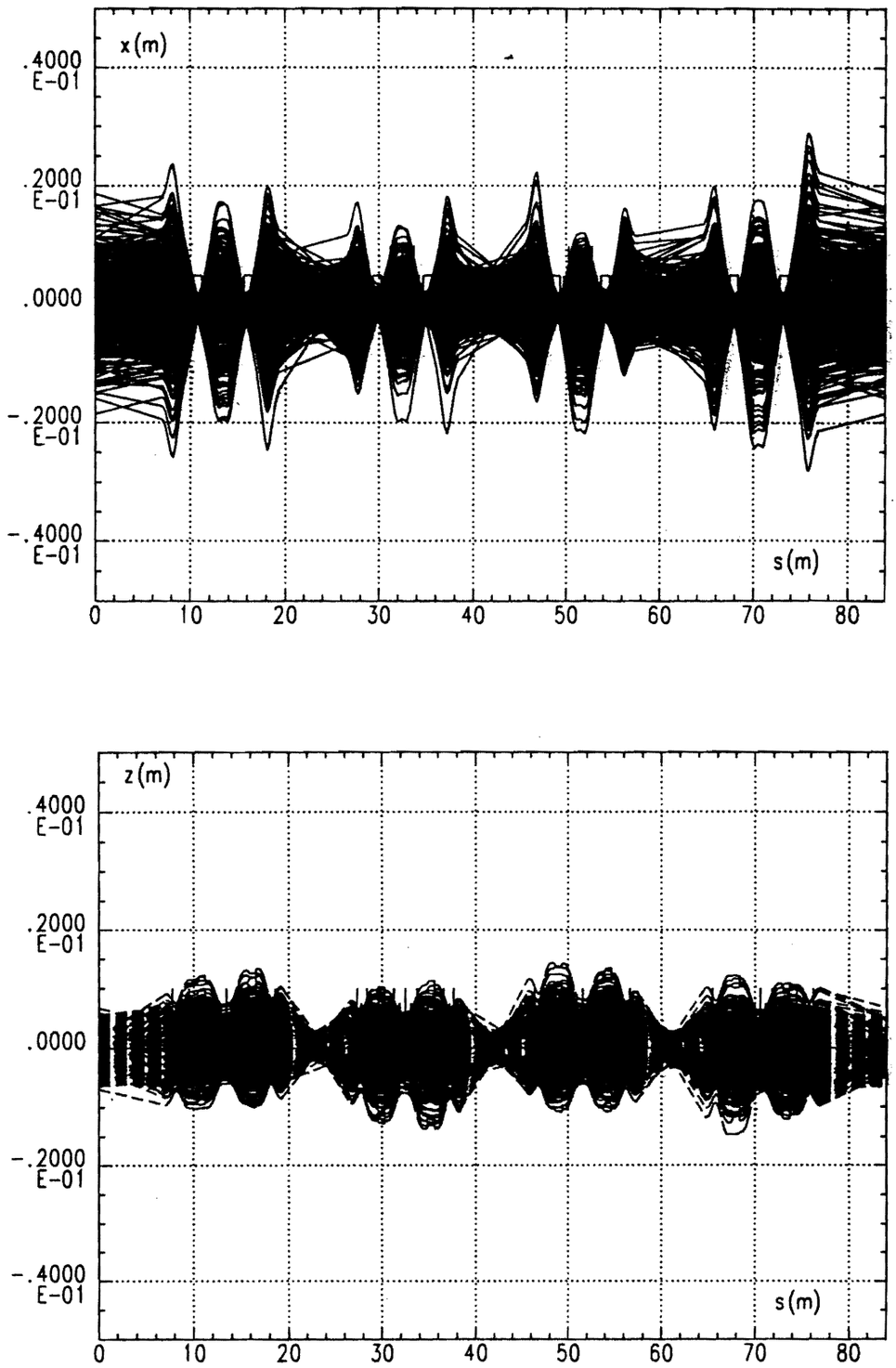

Fig. 9 : Closed orbit excursions with dipolar errors for the operating point $\varepsilon_x = 2.7$ nm.rad.

The statistic study (over 100 samples of errors) showed that for all the operating points, 90 % of the closed orbits are smaller than ± 20 mm in x-plan and ± 15 mm in z-plan.

The maximum tune shifts (given as r.m.s. values) are $\sigma(\Delta\nu_x) = 0.036$ and $\sigma(\Delta\nu_z) = 0.035$ and the reduction of the dynamic aperture is severe in some cases as shown on **figure 10** for the operating point $\varepsilon_x = 2.7$ nm.rad for 10 samples.

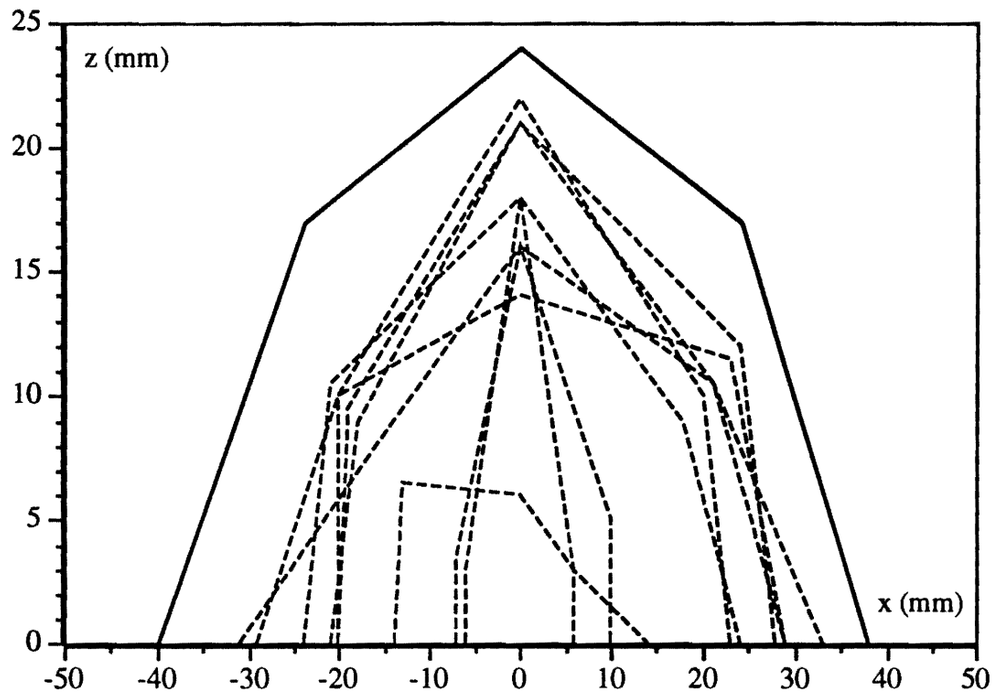

Fig. 10 : Effect of dipolar errors on the dynamic aperture (calculated over 100 turns) for the operating point $\varepsilon_x = 2.7$ nm.rad.

If the defaults on quadrupole positionning can be reduced to 5 10^{-5} m, then the closed orbit excursions are reduced to x = ± 15 mm and z = ± 10 mm (for 99 % of samples) and the dynamic aperture is almost recovered (**figure 11**).

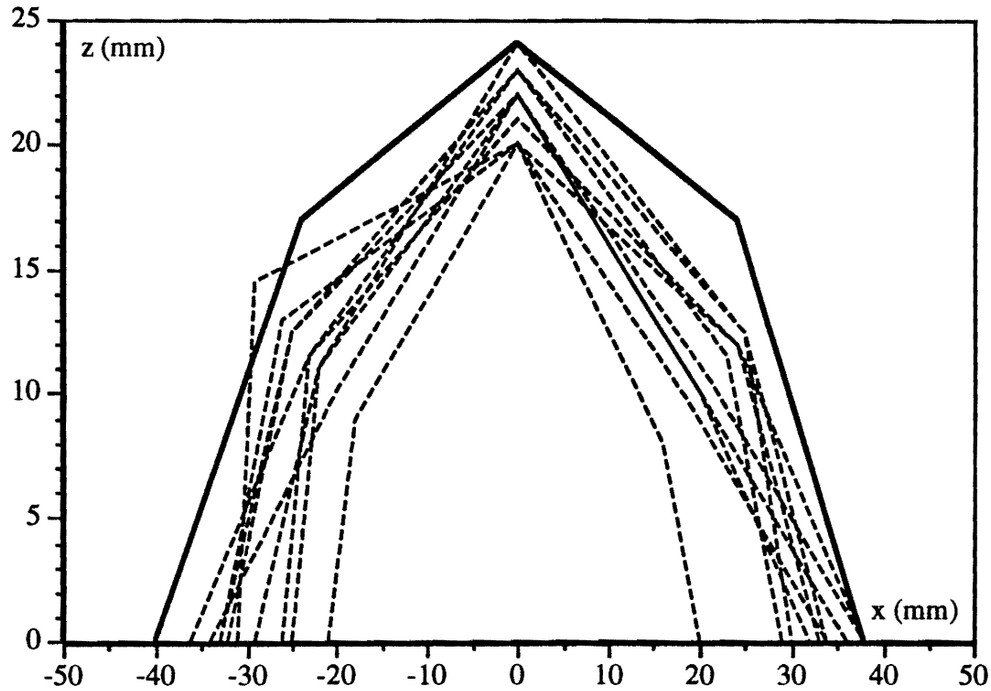

Fig. 11 : Dynamic aperture (calculated over 100 turns) with quadrupole positionning errors reduced to 5 10^{-5} m for the operating point ε_x = 2.7 nm.rad.

3) Sensitivity to focusing errors

In addition to dipolar errors, the main sources for focusing errors are gradient errors in quadrupoles and horizontal mispositionning of sextupoles. The study of the effect of these errors for the nominal points led to the following tolerances given as r.m.s. values [10] :

- Integrated gradient error :
  - quadrupoles : $\sigma(G\ell)/(G\ell)_0 = 1\ 10^{-3}$
- Alignment error :
  - sextupoles : $\sigma_x = 1\ 10^{-4}$ m

The modulation of optical functions and the tune shifts are then (r.m.s. values) :

- gradient errors :	$\sigma(\Delta\beta_y/\beta_y)$	= 5 %	(y = x or z)
	$\sigma(\Delta\nu_x)$	= 0.010	
	$\sigma(\Delta\nu_z)$	= 0.007	
- sextupole positionning errors :	$\sigma(\Delta\beta_y/\beta_y)$	= 4 %	(y = x or z)
	$\sigma(\Delta\nu_x)$	= 0.007	
	$\sigma(\Delta\nu_z)$	= 0.007	

The reduction of the dynamic aperture is negligible and the resulting closed orbit is smaller than 0.05 mm.

4) Sensitivity to multipolar field components

The individual effect of each multipolar field component has been computed, and the maximum values retained as tolerances are the ones which keep the dynamic aperture almost unchanged [11, 12].

The tolerances are evaluated at the limit of the good field region which is $\Delta x = \pm 20$ mm in the dipoles and $\Delta x = \pm 40$ mm in the quadrupoles (this region is defined by the injection study, see section **5**).

The following components have been studied :

Multipolar component	In Dipole	In Quadrupole
Quadrupolar	Systematic	
Sextupolar	Systematic	Random
Octupolar	Systematic	Systematic
Decapolar	Systematic	Random
Dodecapolar		Systematic

The tolerances required to keep the dynamic aperture almost unchanged are given in **Table 4**.

Table 4 : Tolerances on multipolar field components.

DIPOLE : $\Delta B/B$ at $\Delta x = \pm 20$ mm	
Quadrupolar (systematic, random)	$3\ 10^{-4}$, $1\ 10^{-4}$
Sextupolar (systematic, random)	$5\ 10^{-4}$, $5\ 10^{-4}$
Octupolar (systematic, random)	$2\ 10^{-4}$, $2\ 10^{-4}$
Decapolar (systematic, random)	$1\ 10^{-3}$, $5\ 10^{-4}$
QUADRUPOLE : $\Delta G/G$ at $\Delta x = \pm 40$ mm	
Sextupolar (random σ)	$7\ 10^{-4}$
Octupolar (systematic, random)	$5\ 10^{-3}$, $3\ 10^{-3}$
Decapolar (random σ)	$1\ 10^{-3}$
Dodecapolar (systematic, random)	$1\ 10^{-2}$, $3\ 10^{-3}$

The effect of all these components on the dynamic aperture (calculated over 100 turns) is shown on **figure 12** for the operating point ε_x = 2.7 nm.rad.

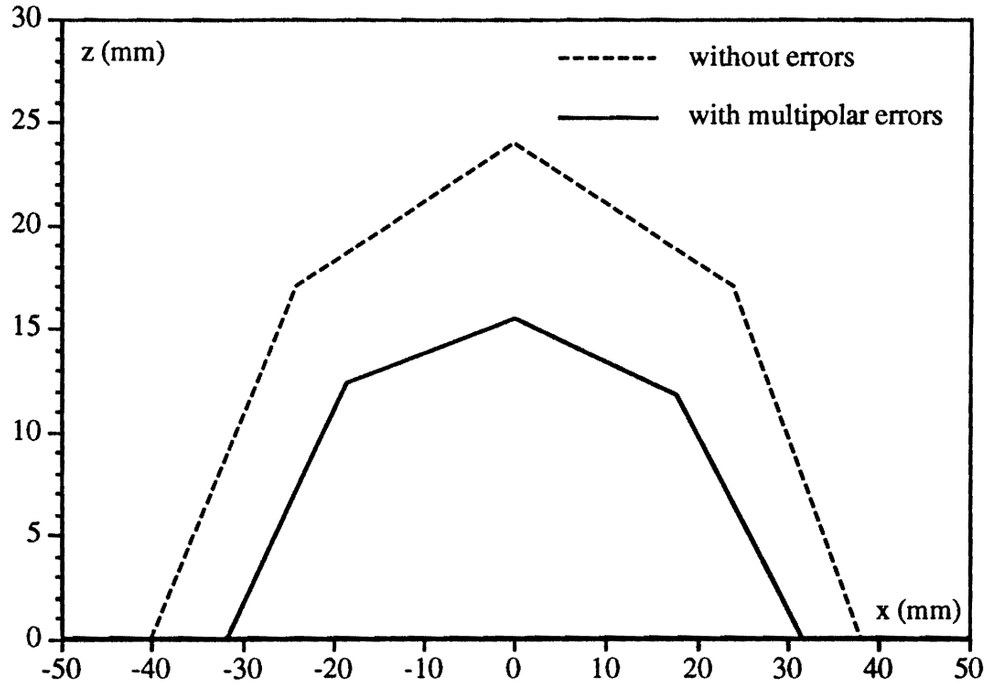

Fig. 12 : Dynamic aperture for the operating point ε_x = 2.7 nm.rad with all systematic and random multipolar field components.

Remarks :

• In the simulation, all multipole components have the same positive sign, which represents the most pessimistic case. When magnetic element calculations will be done, then new computations will be performed with realistic signs, in order to relax, if possible, the tightest tolerances.

• Quadrupolar and sextupolar components of the dipole can be compensated by quadrupoles and sextupoles of the lattice, then the dynamic aperture is almost recovered.

5) Optimization of the injection

The beam is injected from the inside of the ring in one of the 4 long straight sections where the complete injection system is located.

All the operating points have been studied in order to optimize injection parameters as optical functions, number of standard deviations for the injected beam (2.5 σ) and the stored beam (4 σ) and to define the septum position and the vacuum chamber aperture [13].

The transport over 10 turns of the injected phase ellipses (with sextupoles on) has shown that in the optimized situation, the position of the septum, valid for all the operating points, is -18.2 mm. This leads to orbit excursions of $\Delta x = \pm 25$ mm in x-plan and $\Delta z = \pm 7$ mm in z-plan. **Figure 13** and **figure 14** show the tracking results for the operating point $\varepsilon_x = 2.7$ nm.rad.

Taking into account the closed orbit excursion due to dipolar errors ($\Delta x = \pm 15$ mm and $\Delta z = \pm 10$ mm), the good field region should be $\Delta x = \pm 40$ mm and $\Delta z = \pm 17$ mm in the quadrupoles, while $\Delta x = \pm 20$ mm is sufficient in the dipoles.

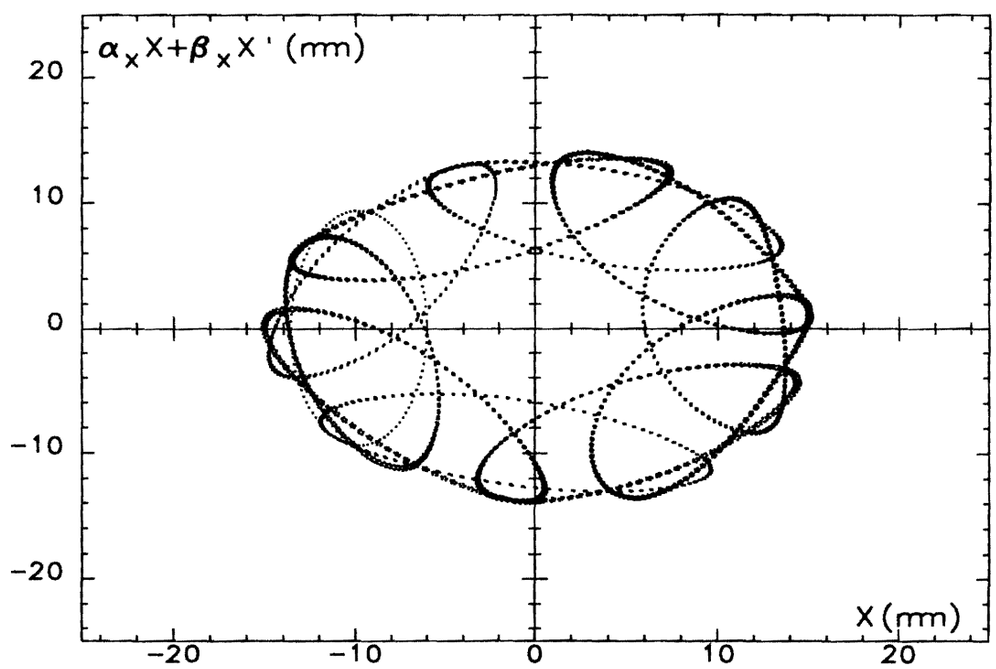

Fig. 13 : Transport over 10 turns of the injected ellipses with sextupoles on.

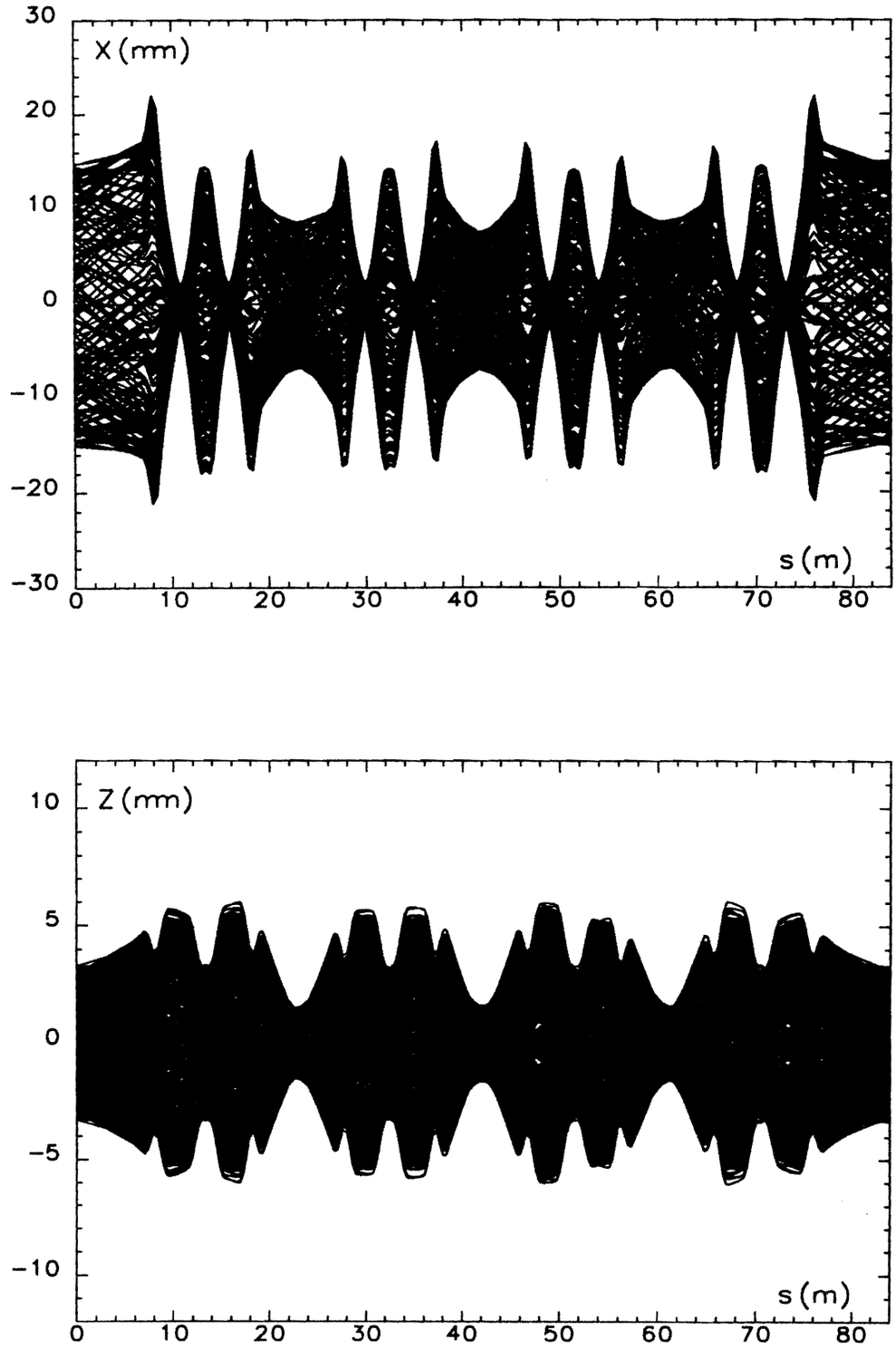

Fig. 14 : Transport of injected particles over 2 turns.

V. BRILLIANCE AND BEAM LIFETIME

1) Brilliance

Figure 15 shows the brilliance calculated at the typical operating point (ε_x = 2.7 nm.rad) with a beam current of 500 mA, and a coupling factor of 1 %, from the bending magnet and several types of insertion devices, covering all the energy range from 10 eV to 100 keV.

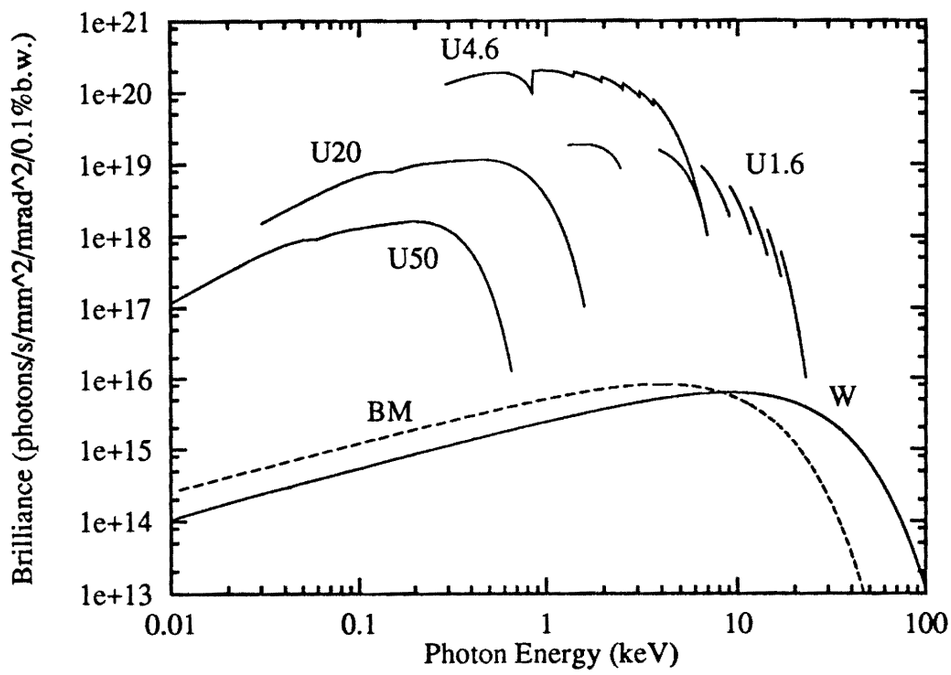

Fig. 15 : Typical brilliance for SOLEIL.

U4.6 :	period = 4.6 cm	N = 150	K_{max} = 2.2
U20 :	period = 20 cm	N = 50	K_{max} = 3.5
U50 :	period = 50 cm	N = 20	K_{max} = 3.9
U1.6 :	period = 1.6 cm	N = 30	K_{max} = 1.5
W :	1 pole superconducting wiggler B_{max} = 3.5 T		

• The maximum brilliance at about 2 10^{20} ph/s/mm^2/mrad^2/0.1 % $\Delta\lambda/\lambda$, is obtained around 1 keV with a 7 m long undulator located in the shorter straight section.

• One of the four 14 m long straight sections is dedicated to the FEL (in the 350 - 100 nm energy range) designed for experimental use and especially for pump-probe experiments. The other two free long straight sections are open for future developments : at the moment, very long undulators without monochromator (U20, U50) and also several undulators with different magnetic axis (magnetic chicane) are considered.

• In the high energy range, wavelength shifters (single pole superconducting wigglers) are foreseen and short minigap undulators (U1.6) are under study.

2) Beam lifetime

Three modes of operation are expected :

1) High brilliance at 2.15 GeV with 500 mA.
2) Temporal structure at 2.15 GeV with 8 x 10 mA.
3) FEL compatible with temporal structure at 1.5 GeV with 8 x 10 mA.

Beam gas (τ_v) and Touschek lifetimes have been computed for different emittance, coupling and energy values with the following parameters :

• The pressure is 10^{-9} Torr for 500 mA and 2 10^{-10} Torr for 80 mA.

• The maximum RF voltage is chosen in order to provide an energy acceptance of 4 % (cf. part **IV.1, Table 2**).

Table 5 shows the results for the three modes of operation, the values in bold type correspond to beam lifetime larger than 10 h and maximum factor of merit (brilliance x beam lifetime).

Table 5 : Beam lifetime for three modes of operation.

E (GeV)	2.15		1.5
ε_x (nm.rad)	2.7		15
I (mA)	500	8 x 10	8 x 10
τ_v(h)	33	164	115
κ^2 τ_T(h) ; τ_{tot} (h)			
0.01	20 ; **12.5**	2 ; 2	3 ; 3
0.10	63 ; 22	6 ; 6	9 ; 8
1	138 ; 27	12 ; **11**	16 ; **14**

Nota :

• These calculations do not take into account the effects of insertion devices. Simulations of these effects are under way.

• For the high brilliance mode, Touschek lifetime was calculated with 560 bunches. If a gap in the bunch train is necessary to avoid ions or dust particles trapping, this lifetime will be reduced in the same way.

VI. CONCLUSION

The SOLEIL parameters optimized in order to reach the targets, are presently completely defined and the ultra vacuum and magnetic element systems detailed studies are now in progress.

The machine offers very high performances at 2.15 GeV with extremely high brilliance from undulators as well as at 1.5 GeV with the FEL providing the possibility of two color experiments as already shown on Super-ACO [14].

SOLEIL associated with the ETOILES project [15], which would cover the whole infrared domain with synchronized FEL, will be a unique multipurpose high performance tool.

VII. ACKNOLEDGMENT

We are indebted to J.-L. Laclare for fruitful discussions on the machine parameters, M.-E. Couprie and P. Thiry for their implication as designers of insertions and experiments.

VIII. REFERENCES

[1] M.-P. Level et al., "SOLEIL, a New Synchrotron Radiation Source for LURE", PAC 93, Vol. 2, p 1465.

[2] P. Brunelle et al., "New Optics for SOLEIL", EPAC 94, Vol. 1, p 615.

[3] M.-E. Couprie et al., "Projet SOLEIL, Argumentation Scientifique", Les Editions de Physique, Juin 1993, p 257.

[4] J. Payet et al., to be published.

[5] P. Nghiem, J. Payet, A. Tkatchenko, "Structure, réglages et performances d'un anneau à 4 superpériodes pour SOLEIL", Note/S/95-03.

[6] P. Brunelle, A. Nadji, "Réglage et performances de SOLEIL pour l'émittance 30 nm.rad", rapport APD SOLEIL/A/95-08.

[7] P. Brunelle, A. Nadji, "Acceptance dynamique à chromaticité verticale élevée", rapport APD SOLEIL/A/95-06.

[8] P. Nghiem, "Effet des défauts dipolaires sur l'optique de SOLEIL", Note/S/95-04.

[9] P. Nghiem et al., to be published.

[10] P. Brunelle, A. Nadji, "Sensibilité aux défauts de focalisation", rapport APD SOLEIL/A/95-05.

[11] P. Brunelle, A. Nadji, "Tolérances sur les composantes multipolaires des dipôles et des quadrupôles de SOLEIL", rapport APD SOLEIL/A/95-02.

[12] P. Brunelle, A. Nadji, "Etude complémentaire sur les tolérances multipolaires des dipôles et quadrupôles de SOLEIL", rapport APD SOLEIL/A/95-10.

[13] J. Payet, "Paramètres de l'injection dans l'Anneau", Note/S/95-05.

[14] M.-E. Couprie, "Applications of FELs in the UV", proceedings of the "Symposium on Ion and Laser Processing for Advanced Materials", Oct. 1994, Keihanna, edited by T. Takagi and T. Tomimasu, pp. 181-186.

[15] J.-M. Ortega et al., "Le Projet ETOILES", to be published.

Appendix A

Table A shows the main optical characteristics of the eleven operating points where :

- ε_x is the horizontal emittance,
- ν_x and ν_z are horizontal and vertical tunes,
- ξ_x and ξ_z are horizontal and vertical natural chromaticities defined as $\xi = \frac{(\Delta\nu / \nu)}{(\Delta p / p)}$,
- β_x^{max} and β_z^{max} are the maximum values of the optical functions in the lattice.

Table A.

Parameters / Operating Points	ε_x (nm.rad)	ν_x	ν_z	ξ_x	ξ_z	β_x^{max} (m)	β_z^{max} (m)
1	6.83	19.69	7.62	-3.77	-3.58	35.5	25.4
2	5.07	19.30	7.38	-3.01	-3.01	28.4	21.0
3	6.84	17.69	7.77	-3.89	-3.68	34.0	24.0
4	4.08	17.69	7.77	-3.37	-3.42	30.3	24.3
5	2.98	17.69	7.76	-3.31	-3.46	30.0	24.7
6	2.39	17.70	7.77	-3.24	-3.38	29.9	24.2
7	7.71	18.30	8.30	-3.27	-2.84	31.0	18.4
8	2.71	18.30	8.38	-2.98	-2.90	30.4	18.9
9	8.24	18.21	8.27	-3.08	-2.22	30.0	15.7
10	4.03	18.22	8.27	-2.93	-2.18	30.0	15.5
11	2.49	18.19	8.33	-3.07	-2.72	29.8	18.6

Table B gives the maximum brilliance from undulators (in unit of "photons/s/mm^2/mrad^2/0.1 % $\Delta\lambda/\lambda$") for the eleven operating points, using the following parameters :

- stored beam : I = 500 mA
  κ^2 (coupling) = 1 %

- undulators : [K = 93.4 B(T) λ(m)], K_{min} = 0.5 ; K_{max} = 2.178

  U1 : 220 periods of 0.046 m in the long straight section.
  U2 : 150 periods of 0.046 m in the first medium straight section.
  U3 : 150 periods of 0.046 m in the second medium straight section.

Table B.

Brilliance from / Operating Points	U1	U2	U3
1	0.86	0.89	0.89
2	1.17	1.04	0.96
3	0.64	0.91	0.90
4	1.34	1.51	1.51
5	1.76	1.95	1.94
6	1.96	2.12	2.09
7	0.73	0.78	0.78
8	2.01	1.81	1.73
9	0.68	0.65	0.52
10	1.45	1.35	1.13
11	1.88	1.90	1.64

ERRATA

Page 6 : The dimensions at source points for the 15 nm.rad operating point are computed with **K^2 = 100 %** coupling factor.

Page 22 : **Table B** gives the maximum brilliance from undulators (in unit of "**10^{20}** photons/s/mm^2/mrad^2/0.1 % $\Delta\lambda/\lambda$) for the eleven operating points, using the following parameters :